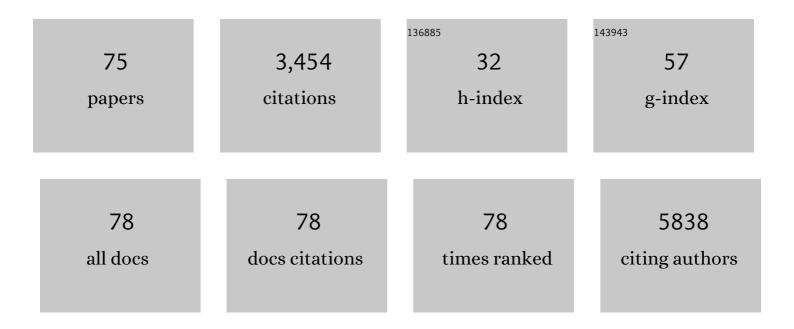
List of Publications by Year in descending order

Source: https://exaly.com/author-pdf/882772/publications.pdf Version: 2024-02-01



#	Article	IF	CITATIONS
1	Efficient, stable silicon tandem cells enabled by anion-engineered wide-bandgap perovskites. Science, 2020, 368, 155-160.	6.0	420
2	<b>An Ultrahighâ€Performance Photodetector based on a Perovskite–Transitionâ€Metalâ€Dichalcogenide Hybrid Structure</b> . Advanced Materials, 2016, 28, 7799-7806.	11.1	242
3	The Role of Sodium as a Surfactant and Suppressor of Nonâ€Radiative Recombination at Internal Surfaces in Cu <sub>2</sub> ZnSnS <sub>4</sub> . Advanced Energy Materials, 2015, 5, 1400849.	10.2	186
4	A Distributed Model for Border Traps in \$hbox{Al}_{2} hbox{O}_{3}-hbox{InGaAs}\$ MOS Devices. IEEE Electron Device Letters, 2011, 32, 485-487.	2.2	162
5	Origin and passivation of fixed charge in atomic layer deposited aluminum oxide gate insulators on chemically treated InGaAs substrates. Applied Physics Letters, 2010, 96, .	1.5	148
6	Laser Crystallization of Organic–Inorganic Hybrid Perovskite Solar Cells. ACS Nano, 2016, 10, 7907-7914.	7.3	123
7	Amorphizing noble metal chalcogenide catalysts at the single-layer limit towards hydrogen production. Nature Catalysis, 2022, 5, 212-221.	16.1	113
8	Effects of a SnO <sub>2</sub> hole blocking layer in a BiVO <sub>4</sub> -based photoanode on photoelectrocatalytic water oxidation. Journal of Materials Chemistry A, 2017, 5, 6905-6913.	5.2	107
9	Stability of Halide Perovskite Solar Cell Devices: In Situ Observation of Oxygen Diffusion under Biasing. Advanced Materials, 2018, 30, e1802769.	11.1	92
10	Unbiased biocatalytic solar-to-chemical conversion by FeOOH/BiVO4/perovskite tandem structure. Nature Communications, 2018, 9, 4208.	5.8	83
11	Continuous 3D Titanium Nitride Nanoshell Structure for Solarâ€Đriven Unbiased Biocatalytic CO <sub>2</sub> Reduction. Advanced Energy Materials, 2019, 9, 1900029.	10.2	81
12	Extremely Low Contact Resistance on Graphene through nâ€īype Doping and Edge Contact Design. Advanced Materials, 2016, 28, 864-870.	11.1	70
13	Improving the openâ€circuit voltage of Cu <sub>2</sub> ZnSnSe <sub>4</sub> thin film solar cells via interface passivation. Progress in Photovoltaics: Research and Applications, 2017, 25, 308-317.	4.4	66
14	Carrier-resolved photo-Hall effect. Nature, 2019, 575, 151-155.	13.7	66
15	Hybrid Perovskites: Effective Crystal Growth for Optoelectronic Applications. Advanced Energy Materials, 2017, 7, 1602596.	10.2	62
16	Microstructural Evolution of Hybrid Perovskites Promoted by Chlorine and its Impact on the Performance of Solar Cell. Scientific Reports, 2019, 9, 4803.	1.6	61
17	Pre-atomic layer deposition surface cleaning and chemical passivation of (100) In0.2Ga0.8As and deposition of ultrathin Al2O3 gate insulators. Applied Physics Letters, 2008, 93, .	1.5	60
18	Compositional engineering of solution-processed BiVO4 photoanodes toward highly efficient photoelectrochemical water oxidation. Nano Energy, 2018, 43, 244-252.	8.2	57

#	Article	IF	CITATIONS
19	Atomic‣cale Observation of Oxygen Substitution and Its Correlation with Holeâ€Transport Barriers in Cu <sub>2</sub> ZnSnSe <sub>4</sub> Thinâ€Film Solar Cells. Advanced Energy Materials, 2016, 6, 1501902.	10.2	56
20	Effects of the incorporation of alkali elements on Cu(In,Ga)Se2 thin film solar cells. Solar Energy Materials and Solar Cells, 2016, 157, 695-702.	3.0	53
21	Understanding effects of precursor solution aging in triple cation lead perovskite. RSC Advances, 2018, 8, 21551-21557.	1.7	53
22	Preparation of single-phase SnSe thin-films and modification of electrical properties via stoichiometry control for photovoltaic application. Journal of Alloys and Compounds, 2017, 722, 474-481.	2.8	50
23	Improving Uniformity and Reproducibility of Hybrid Perovskite Solar Cells via a Low-Temperature Vacuum Deposition Process for NiO <i><sub>x</sub></i> Hole Transport Layers. ACS Applied Materials & Interfaces, 2018, 10, 534-540.	4.0	49
24	Reduced Graphene Oxide as a Catalyst Binder: Greatly Enhanced Photoelectrochemical Stability of Cu(In,Ga)Se <sub>2</sub> Photocathode for Solar Water Splitting. Advanced Functional Materials, 2018, 28, 1705136.	7.8	46
25	Aminosilaneâ€Modified CuGaO <sub>2</sub> Nanoparticles Incorporated with CuSCN as a Holeâ€Transport Layer for Efficient and Stable Perovskite Solar Cells. Advanced Materials Interfaces, 2019, 6, 1901372.	1.9	43
26	Passivation of Deep-Level Defects by Cesium Fluoride Post-Deposition Treatment for Improved Device Performance of Cu(In,Ga)Se <sub>2</sub> Solar Cells. ACS Applied Materials & Interfaces, 2019, 11, 35653-35660.	4.0	41
27	Effects of temperature and coating speed on the morphology of solution-sheared halide perovskite thin-films. Journal of Materials Chemistry A, 2018, 6, 24911-24919.	5.2	40
28	Bias-Free In Situ H <sub>2</sub> O <sub>2</sub> Generation in a Photovoltaic-Photoelectrochemical Tandem Cell for Biocatalytic Oxyfunctionalization. ACS Catalysis, 2019, 9, 10562-10566.	5.5	40
29	Uniform Cs2SnI6 Thin Films for Lead-Free and Stable Perovskite Optoelectronics via Hybrid Deposition Approaches. Electronic Materials Letters, 2019, 15, 192-200.	1.0	38
30	Understanding the Origin of Ultrasharp Sub-bandgap Luminescence from Zero-Dimensional Inorganic Perovskite Cs <sub>4</sub> PbBr <sub>6</sub> . ACS Applied Energy Materials, 2020, 3, 192-199.	2.5	36
31	Tailoring Photoelectrochemical Performance and Stability of Cu(In,Ga)Se <sub>2</sub> Photocathode via TiO <sub>2</sub> -Coupled Buffer Layers. ACS Applied Materials & Interfaces, 2017, 9, 5279-5287.	4.0	34
32	Arsenic decapping and half cycle reactions during atomic layer deposition of Al2O3 on In0.53Ga0.47As(001). Applied Physics Letters, 2010, 96, .	1.5	33
33	Modulation of Growth Kinetics of Vacuum-Deposited CsPbBr <sub>3</sub> Films for Efficient Light-Emitting Diodes. ACS Applied Materials & Interfaces, 2020, 12, 1944-1952.	4.0	33
34	Unassisted Water Splitting Exceeding 9% Solar-to-Hydrogen Conversion Efficiency by Cu(In, Ga)(S, Se)2 Photocathode with Modified Surface Band Structure and Halide Perovskite Solar Cell. ACS Applied Energy Materials, 2020, 3, 2296-2303.	2.5	31
35	Extraordinary Enhancement of UV Absorption in TiO <sub>2</sub> Nanoparticles Enabled by Low-Oxidized Graphene Nanodots. Journal of Physical Chemistry C, 2018, 122, 12114-12121.	1.5	30
36	Strategies to reduce the open-circuit voltage deficit in Cu2ZnSn(S,Se)4 thin film solar cells. Electronic Materials Letters, 2017, 13, 373-392.	1.0	28

#	Article	IF	CITATIONS
37	Meniscus-Guided Control of Supersaturation for the Crystallization of High Quality Metal Organic Framework Thin Films. Chemistry of Materials, 2019, 31, 7377-7385.	3.2	28
38	Robust FeOOH/BiVO <sub>4</sub> /Cu(In, Ga)Se <sub>2</sub> tandem structure for solar-powered biocatalytic CO <sub>2</sub> reduction. Journal of Materials Chemistry A, 2020, 8, 8496-8502.	5.2	28
39	CO <sub>2</sub> â€Reductive, Copper Oxideâ€Based Photobiocathode for Zâ€Scheme Semiâ€Artificial Leaf Structure. ChemSusChem, 2020, 13, 2940-2944.	3.6	27
40	Wet Pretreatment-Induced Modification of Cu(In,Ga)Se <sub>2</sub> /Cd-Free ZnTiO Buffer Interface. ACS Applied Materials & Interfaces, 2018, 10, 20920-20928.	4.0	26
41	Effects of Postsynthesis Thermal Conditions on Methylammonium Lead Halide Perovskite: Band Bending at Grain Boundaries and Its Impacts on Solar Cell Performance. Journal of Physical Chemistry C, 2016, 120, 21330-21335.	1.5	25
42	Lignin-fueled photoelectrochemical platform for light-driven redox biotransformation. Green Chemistry, 2020, 22, 5151-5160.	4.6	24
43	Low-dimensional formamidinium lead perovskite architectures <i>via</i> controllable solvent intercalation. Journal of Materials Chemistry C, 2019, 7, 3945-3951.	2.7	23
44	Tailoring the Mesoscopic TiO2 Layer: Concomitant Parameters for Enabling High-Performance Perovskite Solar Cells. Nanoscale Research Letters, 2017, 12, 57.	3.1	21
45	Sn1â^'xSe thin films with low thermal conductivity: role of stoichiometric deviation in thermal transport. Journal of Materials Chemistry C, 2018, 6, 10083-10087.	2.7	21
46	Densely packed hybrid films comprising SnO <sub>2</sub> and reduced graphite oxide for high-density electrochemical capacitors. Journal of Materials Chemistry A, 2016, 4, 16175-16183.	5.2	20
47	Analysis of vertical phase distribution in reactively sputtered zinc oxysulfide thin films. Applied Surface Science, 2019, 486, 555-560.	3.1	19
48	Tuning the wettability of the blade enhances solution-sheared perovskite solar cell performance. Nano Energy, 2020, 74, 104830.	8.2	19
49	Highly Efficient Vacuum-Evaporated CsPbBr <sub>3</sub> Perovskite Light-Emitting Diodes with an Electrical Conductivity Enhanced Polymer-Assisted Passivation Layer. ACS Applied Materials & Interfaces, 2021, 13, 37323-37330.	4.0	19
50	Emerging Earth-Abundant Solar Absorbers. ACS Energy Letters, 2022, 7, 1553-1557.	8.8	19
51	Surface passivation and point defect control in Cu(In,Ga)Se <sub>2</sub> films with a Na <sub>2</sub> S post deposition treatment for higher than 19% CIGS cell performance. Sustainable Energy and Fuels, 2019, 3, 709-716.	2.5	17
52	Aging of a Vanadium Precursor Solution: Influencing Material Properties and Photoelectrochemical Water Oxidation Performance of Solutionâ€Processed BiVO <sub>4</sub> Photoanodes. Advanced Functional Materials, 2020, 30, 1806662.	7.8	16
53	Enhanced sulfurization reaction of molybdenum using a thermal cracker for forming two-dimensional MoS <sub>2</sub> layers. Physical Chemistry Chemical Physics, 2018, 20, 16193-16201.	1.3	15
54	Color tuning in Cu(In,Ga)Se <sub>2</sub> thinâ€film solar cells by controlling optical interference in transparent front layers. Progress in Photovoltaics: Research and Applications, 2020, 28, 798-807.	4.4	14

#	Article	IF	CITATIONS
55	Determining the Chemical Origin of the Photoluminescence of Cesium–Bismuth–Bromide Perovskite Nanocrystals and Improving the Luminescence via Metal Chloride Additives. ACS Applied Energy Materials, 2020, 3, 4650-4657.	2.5	14
56	Universal Passivation Strategy for the Hole Transport Layer/Perovskite Interface via an Alkali Treatment for Highâ€Efficiency Perovskite Solar Cells. Solar Rrl, 2021, 5, 2000793.	3.1	14
57	Importance of Fine Control of Se Flux for Improving Performances of Sb <sub>2</sub> Se <sub>3</sub> Solar Cells Prepared by Vapor Transport Deposition. Solar Rrl, 2021, 5, 2100327.	3.1	14
58	Chemical Consequences of Alkali Inhomogeneity in Cu <sub>2</sub> ZnSnS <sub>4</sub> Thinâ€Film Solar Cells. Advanced Energy Materials, 2015, 5, 1500922.	10.2	13
59	Influence of hydrogen and oxygen on the structure and properties of sputtered magnesium zirconium oxynitride thin films. Journal of Materials Chemistry A, 2020, 8, 9364-9372.	5.2	11
60	Monodisperse Carbon Nitride Nanosheets as Multifunctional Additives for Efficient and Durable Perovskite Solar Cells. ACS Applied Materials & Interfaces, 2021, 13, 61215-61226.	4.0	9
61	Enhanced electrical conductivity of transparent electrode using metal microfiber networks for gridless thin-film solar cells. Solar Energy Materials and Solar Cells, 2019, 200, 109998.	3.0	8
62	Atomistic consideration of earth-abundant chalcogenide materials for photovoltaics: Kesterite and beyond. Journal of Materials Research, 2018, 33, 3986-3998.	1.2	7
63	Rationally Designed Window Layers for High Efficiency Perovskite/Si Tandem Solar Cells. Advanced Optical Materials, 2021, 9, 2100788.	3.6	7
64	Drop asted Platinum Nanocube Catalysts for Hydrogen Evolution Reaction with Ultrahigh Mass Activity. ChemSusChem, 2021, 14, 2585-2590.	3.6	6
65	Highly Efficient and Stable Iridium Oxygen Evolution Reaction Electrocatalysts Based on Porous Nickel Nanotube Template Enabling Tandem Devices with Solarâ€ŧoâ€Hydrogen Conversion Efficiency Exceeding 10%. Advanced Science, 2022, 9, e2104938.	5.6	6
66	Photoluminescence study of high energy proton irradiation on Cu(In,Ga)Se2 thin films. Thin Solid Films, 2016, 603, 134-138.	0.8	5
67	Review on light absorbing materials for unassisted photoelectrochemical water splitting and systematic classifications of device architectures. Discover Materials, 2022, 2, .	1.0	5
68	Enhancement mode In0.53Ga0.47As MOSFET with self-aligned epitaxial source/drain regrowth. , 2009, , .		4
69	Operando Injection of Oxygen Ions to Organometal Halide Perovskite (CH <sub>3</sub> NH <sub>3</sub> PM <sub>3</sub> ) under <i>In-Situ</i> Electrical Biasing STEM-EELS. Microscopy and Microanalysis, 2017, 23, 1976-1977.	0.2	4
70	Potassium Hydroxide Mixed with Lithium Hydroxide: An Advanced Electrolyte for Oxygen Evolution Reaction. Solar Rrl, 2019, 3, 1900195.	3.1	4
71	Improving Uniformity and Reproducibility of Photoelectrochemical Water Oxidation Performance of BiVO <sub>4</sub> Photoanodes via Selective Removal of Excess V <sub>2</sub> O <sub>5</sub> by Electrochemical Etching. ACS Applied Energy Materials, 2020, 3, 7756-7763.	2.5	4
72	Graphene: Extremely Low Contact Resistance on Graphene through nâ€Type Doping and Edge Contact Design (Adv. Mater. 5/2016). Advanced Materials, 2016, 28, 975-975.	11.1	2

#	Article	IF	CITATIONS
73	Thinâ€Film Solar Cells: Atomicâ€Scale Observation of Oxygen Substitution and Its Correlation with Holeâ€Transport Barriers in Cu <sub>2</sub> ZnSnSe <sub>4</sub> Thinâ€Film Solar Cells (Adv. Energy) Tj ETQq1	<b>110.2</b> 8431	.4 rgBT /O∖
74	0.37 mS/μm In <sub>0.53</sub> Ga <sub>0.47</sub> As MOSFET with 5 nm channel and self-aligned epitaxial raised source/drain. , 2009, , .		0
75	Indentation-induced cracking behavior of a Cu(In,Ga)Se2 films on Mo substrate. Journal of Materials Research and Technology, 2021, 13, 1132-1138.	2.6	0